

Bioceramics: Materials and Applications III

Edited by

Laurie George

Richard P. Rusin

Gary S. Fischman

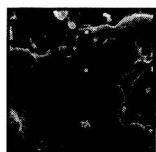
Vic Janas

Ceramic
Transactions
Volume 110

2318-08-53

B615.2

1999



Ceramic
Transactions
Volume 110

Bioceramics: Materials and Applications III

Edited by

Laurie George

American Dental Association Health Foundation

Richard P. Rusin

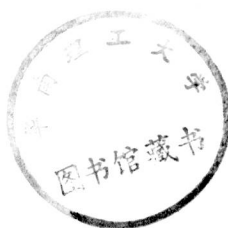
3M Corporation

Gary S. Fischman

University of Illinois

Vic Janas

Johnson & Johnson



E200000813

Published by

The American Ceramic Society

735 Ceramic Place

Westerville, Ohio 43081

Proceedings of the Bioceramics: Materials and Applications symposium, held at the 101st Annual Meeting of The American Ceramic Society, Indianapolis, Indiana, April 25–28, 1999.

Copyright 2000, The American Ceramic Society. All rights reserved.

Statements of fact and opinion are the responsibility of the authors alone and do not imply an opinion on the part of the officers, staff, or members of The American Ceramic Society. The American Ceramic Society assumes no responsibility for the statements and opinions advanced by the contributors to its publications or by the speakers at its programs. Registered names and trademarks, etc., used in this publication, even without specific indication thereof, are not to be considered unprotected by the law.

No part of this book may be reproduced, stored in a retrieval system, or transmitted in any form or by any means, electronic, mechanical, photocopying, microfilming, recording, or otherwise, without written permission from the publisher.

Authorization to photocopy for internal or personal use beyond the limits of Sections 107 and 108 of the U.S. Copyright Law is granted by the American Ceramic Society, provided that the appropriate fee is paid directly to the Copyright Clearance Center, Inc., 222 Rosewood Drive, Danvers, MA 01923 USA, www.copyright.com. Prior to photocopying items for educational classroom use, please contact Copyright Clearance Center, Inc.

This consent does not extend to copying items for general distribution or for advertising or promotional purposes or to republishing items in whole or in part in any work in any format.

Please direct republication or special copying permission requests to Copyright Clearance Center, Inc., 222 Rosewood Drive, Danvers, MA 01923 USA 978-750-8400; www.copyright.com.

COVER PHOTO: "Ca-phosphate coating applied to the surface of zirconia ceramics by plasma coating," is courtesy of J. Cihlar, M. Jez, K. Castkova, and M. Trunec, and appears as figure 3 in their paper "Oxide Ceramics with Calcium Phosphate Coatings," which begins on page 157.

Library of Congress Cataloging-in-Publication Data

A CIP record for this book is available from the Library of Congress.

For information on ordering titles published by The American Ceramic Society, or to request a publications catalog, please call 614-794-5890.

Printed in the United States of America.

4 3 2 1-03 02 01 00

ISSN 1042-1122

ISBN 1-57498-102-1

Bioceramics: Materials and Applications III

Related titles published by The American Ceramic Society:

Surface Active Materials (Ceramic Transactions Volume 101)

Edited by David E. Clark, Joseph Simmons, and Catherine Simmons

©2000, ISBN 1-57498-079-3

Bioceramics: Materials and Applications II (Ceramic Transactions Volume 63)

Edited by Richard P. Rusin and Gary S. Fischman

©1996, ISBN: 1-57498-006-8

Bioceramics: Materials and Applications (Ceramic Transactions Volume 48)

Edited by Gary Fischman, Alexis Clare, and Larry Hench

©1995, ISBN: 0-944904-82-3

For information on ordering titles published by The American Ceramic Society, or to request a publications catalog, please contact our Customer Service Department at 614-794-5890 (phone), 614-794-5892 (fax), <customersrvc@acers.org> (e-mail), or write to Customer Service Department, 735 Ceramic Place, Westerville, OH 43081, USA.

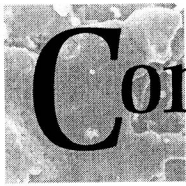
Visit our on-line book catalog at <www.ceramics.org>.



Preface

This symposium on bioceramics is the seventh in a series that looks at biomedical materials from a ceramics perspective. This symposium was sponsored by NICE and the Engineering Ceramics and Glass and Optical Materials divisions of The American Ceramic Society. The program was held at the 101st Annual Meeting of The American Ceramic Society in Indianapolis, Indiana, April 25–28, 1999, under the title "Bioceramics: Materials and Applications." Fifty-seven oral and poster presentations were made.

Laurie George
Richard P. Rusin
Gary S. Fischman
Vic Janas



Contents

Preface	viii
<i>In Vitro</i> Stability Predictions for the Bone/Bioglass and Bone/HA Interactions	I
Melissa J. Crimp, Dean A. Oppermann, and Udhav U. Doctor	
Glass-Hydroxyapatite Coatings on Titanium-Based Implants	15
J.M. Gomez-Vega, E. Saiz, and A.P. Tomsia, G.W. Marshall, and S.J. Marshall	
Synthesis of Hydroxyapatite via Mechanical Activation	25
K.C.B. Yeong, J. Wang, and S.C. Ng	
Preparation of Biomimetic HA Precursors at 37°C in Urea- and Enzyme Urease-Containing Synthetic Body Fluids	39
Defne Bayraktar and A. Cüneyt Tas	
Physical Characteristics of Sintered Hydroxyapatite	53
T.P. Hoepfner and E.D. Case	
Spray Dried Titania Cell Carriers	67
K.-L. Eckert, E. Wintermantel, and R. Gadow	
Crystallization of SiC on Biological Carbon Precursors	81
H. Sieber, H. Friedrich, A. Kaindl, and P. Greil	
Surface Properties of Layered Double Hydroxide Nanocomposites	93
O.C. Wilson Jr., T. Olorunloyemi, A. Jaworski, L. Borum, D. Young, E. Dickens, and C. Oriakhi	
Near-Net-Shape Forming Technique for Bioceramic Components	103
A. Salomoni, I. Stamenkovic, L. Esposito, and A. Tucci	
<i>In Vitro</i> Bioresorbable Fiber Dissolution	113
S.H. Lee and A.G. Clare	
Scope of Piezoelectric Devices in Determining Inner Ear Function	129
N. Mukherjee, R.D. Roseman, and J.P. Willging	

Characterization of Plasma Sprayed HA/ZrO₂ Composite Coatings	145
L. Fu, K.A. Khor, V.J.P. Lim	
Oxide Ceramics with Calcium Phosphate Coatings	157
J. Cihlar, M. Jez, K. Castkova, and M. Trunec	
Processing, Biocompatibility and Biomechanical Testing of Porous Alumina Ceramics	167
Susmita Bose, Jens Darsell, Lihua Yang, Dipak K. Sarkar, and Amit Bandyopadhyay	
Development of Bioceramic Tissue Scaffold via Fused Deposition of Ceramics	183
Iván A. Comejo, Thomas F. McNulty, Shelliam Lee, Ernest Bianchi, Stephen C. Danforth, Ahmad Safari, Kevor S. TenHuisen, and Victor F. Janas	
Index	197

IN VITRO STABILITY PREDICTIONS FOR THE BONE/BIOGLASS AND BONE/HA INTERACTIONS

Melissa J. Crimp, Dean A. Oppermann, and Udhav U. Doctor
Department of Materials Science & Mechanics
Michigan State University
East Lansing, MI 48824-1226

ABSTRACT

Electroacoustic measurements of the zeta (ζ) potential as a function of pH were collected and used to probe the nature of ionic contributions on the bond formed between bone and 2 types of Bioglass (45S5 and 52S) and bone and hydroxyapatite (HA). Powders of each of the synthetic materials and wet bone were dispersed into an electrolyte solution comprised of physiologic saline (0.154M NaCl), electroacoustic measurements collected, and the ζ -potential calculated as a function of pH. The ζ -potential and particle size were then used to calculate the stability of the composite dispersion, where stability is the ability of a particulate to remain in suspension unagglomerated. These stability values were then used to predict the homo- (synthetic to synthetic and bone to bone) versus heterocoagulation (synthetic to bone) behaviors for these synthetic/bone systems. *Single* component suspensions of bone and each of the synthetic materials demonstrated stability against agglomeration. Stability calculations predict that the 45S5/bone interaction was unstable for the pH range tested (5-9), the 52S/bone interaction was stable in the same pH range and the HA/bone interaction was unstable in the pH range, including pH 7.4, the normal *in vivo* pH. These results establish one factor responsible for the observed physicochemical bonding between bone and 45S5 Bioglass and bone/HA noted by many in the orthopedic community. In addition, from the standpoint of ionic attraction, the 52S Bioglass/bone system is not as suitable in terms of bonding to bone in comparison to the 45S5 Bioglass/bone system.

INTRODUCTION

Recent advancements in biomaterials technology have resulted from development of surface reactive or bioactive ceramics. Properties and uses for glass-ceramics have been widely documented¹⁻⁶, focusing on the glass ceramics

To the extent authorized under the laws of the United States of America, all copyright interests in this publication are the property of The American Ceramic Society. Any duplication, reproduction, or republication of this publication or any part thereof, without the express written consent of The American Ceramic Society or fee paid to the Copyright Clearance Center, is prohibited.

such as Bioglass and on calcium phosphate ceramics such as hydroxyapatite (HA) and BCP (Biphasic Calcium Phosphate)^{7,8}. These materials are commonly used as coatings for implants or in bone replacement applications and are characterized by their ability to achieve a strong interfacial bond between implant and bone.

Even though excellent bonding of both Bioglass and HA to bone has been well-documented^{9,10}, the mechanisms for this bonding are not completely understood. One explanation of HA's ability to bond to bone is that calcium phosphates such as HA have been shown to be water soluble, containing the same apatite crystal chemistry as the mineral portion of bone. HA dissolves in physiologic solution, re-precipitates on the bone surface, exhibiting epitaxial growth⁹. This leads to the formation of a granular bonding layer between bone and HA¹¹. However, this explanation assumes intimate contact between the HA and the bone upon HA re-precipitation. It is the researchers opinion that this contact and therefore bonding is enhanced by the *in vivo* ionic activity of the HA particles and bone.

Hench attributes the bonding between Bioglasses and bone to kinetic modification of the surface that occurs upon implantation¹². This kinetic modification leads to the formation of a bioactive hydroxylcarbonate (HCA) layer that is structurally and chemically equivalent to the mineral phase of bone. Hench has shown that the collagenous constituent of soft tissues can strongly adhere to Bioglasses. The collagen fibrils are woven into the interface by growth of the HCA layer. The HCA/collagen interface thickness mimics that of tendons and ligaments to bone. Even though the mechanisms for the HCA formation have been well documented the mechanisms for collagen adhesion are not completely understood.

The degree of ionic activity between bone and synthetic materials may be assessed through the zeta (ζ) potential as calculated from the acoustophoretic particle mobility. O'Brien^{13,14} and Oja¹⁵ have extensively described the electrokinetic phenomena of acoustophoresis. Particles suspended in an electrolyte generate an acoustic wave when subjected to an alternating electric field due to any surface charge and density differential between the particles and the liquid ($\Delta\rho$). This acoustic wave is measured as pressure amplitude per unit of applied electric field ($ESA(\omega)$) from which the particle dynamic mobility ($\mu_d(\omega)$) is calculated using an equation derived by O'Brien^{13,14}:

$$\mu_d(\omega) = ESA(\omega) / \phi \Delta \rho c \quad (1)$$

where ϕ is the volume fraction solid and c is the velocity of sound in the suspension. The ζ -potential is calculated using the acoustophoretic mobility with a correction for the particle inertia $G(\alpha)^{-1}$, in an alternating field. This correction reduces the velocity amplitude of particle motion. The equation to calculate the ζ -potential was derived using the Helmholtz-Smoluchowski equation^{13,14}:

$$\zeta = (\mu\eta / \varepsilon_o \varepsilon_r) G(\alpha)^{-1} \quad (2)$$

Where ε_o is the permittivity in a vacuum, ε_r is the relative permittivity, and $G(\alpha)^{-1}$ is given by:

$$G(\alpha)^{-1} = \left[1 - \frac{i\alpha(3 + 2\Delta\rho/\rho)}{9\{1 + (1-i)(\alpha/2)^{1/2}\}} \right]. \quad (3)$$

Colloidal theory has been used extensively in manufacturing ceramics to eliminate agglomeration and segregation¹⁶⁻²⁰ of system components such as second phase reinforcements. Van der Waals, steric, and repulsive forces act on colloidal particles (particle size $\leq 1\mu\text{m}$) to generate either an agglomerated state or a dispersed suspension according to Derjaguin and Landau²¹, and Verwey and Overbeek²² (DLVO) predictions. To describe the effects of homo- and heterocoagulation and to generate a quantitative theory for the overall kinetic stability of a system of non-identical particles, Hogg et al.²³ developed an expression for interparticle stability (W_{ij}). This factor, termed the stability ratio is in effect, the ratio of particle collision to collisions that result in agglomeration.

$$W_{ij} = \int_{a_i + a_j}^{\infty} \exp\left(\frac{V_T}{kT}\right) \frac{dr}{r^2} \quad (4)$$

In Equation 4, the interparticle stability varies exponentially with the total force, V_T , (attractive and repulsive) and inversely with the square of the particle separation distance, r , from a separation equal to the sum of the two particle radii, a_i and a_j to an infinite separation distance into the solution. The repulsive force, which acts as a barrier to coagulation is proportional to the surface charge of the particle²⁴. However, this surface charge is not readily measurable because of continuous ion activity at the particle/fluid interface. Therefore, the surface charge is estimated at the double layer by the ζ -potential which in this study, is measured using electroacoustic (ESA) methods.

EXPERIMENTAL PROCEDURE

Materials

45S5 and 52S Bioglass¹ were used in this study. The Bioglass compositions are given in Table I. The Bioglasses were ground using mortar and pestle and ball milled dry for 48 hours using alumina grinding media prior to ζ -potential measurement.

Stoichiometric HA (Ca/P=1.67) powder was used for this study, with a manufacturers² reported particle size of 25 μm . Each of these powders were subsequently ground using mortar and pestle and wet sieved using distilled, de-

¹ U.S. Biomaterials Corp.

² Aldrich Chemical, Inc.

TABLE I: COMPOSITION OF BIOGLASSES

<u>Component (wt%)</u>	<u>45S5</u>	<u>52S</u>
SiO ₂	45	52
P ₂ O ₅	6	6
CaO	24.5	21
Na ₂ O	24.5	21

ionized water in a RO-TAP³ test sieve. Sequential sieve meshes of 25 μ m, 15 μ m and 5 μ m were employed to guarantee particles of <5 μ m. The resultant powders were each then air dried at 50°C. The HA powder was examined by x-ray analysis using an X-ray Diffractometer⁴ which detected no alterations in the sieved HA crystal structure when compared to the as-received HA powder.

Bone stock came from the femur of a game deer harvested within 2 hours of death and stored at 6°C for 24 hours then frozen at -18°C for 48 hours prior to use. The frozen femoral shaft was then sectioned into 11, 1-cm transverse discs, and the soft tissue removed. Processing time was minimized to maintain the bone in a frozen state. The bone discs were wet ground from the sub-periosteal surface to the mid cortex in physiologic, 0.154M NaCl, saline solution using a silicon carbide conical grinding bit at approximately 6,000 rpm with mild hand pressure. The resulting bone particles were next ball milled for 12 hours under refrigerated (3°C) conditions.

The particle sizes for the HA materials and the bone were measured using a laser scattering particle size distribution analyzer^{5,6}. The particle radius data for all the synthetic materials and the bone are listed in Table II.

Table II: Particle Radius data for Bioglass, HA and bone in 0.154M saline.

<u>Sample</u>	<u>Mean (μm)</u>	<u>Median (μm)</u>
45S5	1.86	2.64
52S	2.6	4.76
HA	1.46	0.96
bone	0.41	0.31

Methods

To simulate *in vivo* ionic activity between the synthetic materials and bone, both the synthetic materials and bone powders were suspended in 0.2 %.

³ Tyler RX-29

⁴ Scintag 2000

⁵ Horiba model LA-910, available at Flint Ink, of Ann Arbor, MI.

⁶ Malvern Master Sizer X, Malvern Instruments Ltd.

0.154 M NaCl solution and dispersed using an ultrasonic probe⁷ at 70W for 2 minutes. The suitability of *in vitro* studies was addressed by Bagambisa et al.⁹ who found that an aqueous *in vitro* model yielded complementary results when compared to the *in vivo* because of the ubiquitous presence of water. ζ -potential measurements for the synthetic materials and bone were made using electrokinetic sonic amplitude (ESA)⁸ techniques and collected as a function of pH. The pH was controlled by automatic burette titration of 1M NaOH or 1M HCl into the continuously stirred particle suspension. The particle parameters used during testing are listed in Table III. The viscosity and dielectric constants for the saline solution were estimated to be that of water, 8.92×10^{-4} Pascal-sec and 78.45, respectively, as there are only negligible differences between the viscosity and dielectric constant for water and low concentrations of NaCl solutions²⁵.

Table III: Bone and HA input data used for ζ -potential determination.

Sample	Density (g/cc)	Particle Radius (μm)
45S5	2.65	1.86
52S	2.65	2.8
HA	3.1	1.46
Bone	2.0	0.41

ζ -potential values at each pH along with the particle size were then used to calculate the stability ratios for homo- and heterocoagulation²⁶. The calculations are based on a constant particle charge assumption, and require the input of the dielectric constants for each medium. These constants are listed in Table IV.

Table IV: Dielectric constant values²⁷⁻²⁹ and the calculated Hamaker constants.

Sample	Dielectric Constant	Hamaker Constant (J)
45S5	6.9	6.5×10^{-19}
52S	6.9	6.5×10^{-19}
HA	4	1.5×10^{-19}
Bone	17	3.6×10^{-19}
Saline	78.36	4.5×10^{-19}

RESULTS

Zeta Potential

The ζ -potential data as a function of pH for the synthetic materials and bone powders in physiologic saline are shown in Figure 1. The ζ -potential for the 45S5 Bioglass varies from 180 (pH 5) to 25 mV (pH 9) while the 52S Bioglass

⁷ Branson Sonifier 250

⁸ Matec ESA-8000

maintains a relatively constant potential of ~ 50 mV in this same pH range. The ζ -potential calculations for the HA powder in physiologic saline showed positive values ranging from 115 to 130mV. The dome-shaped curve, having a maximum ζ -potential at pH 7.0, is similar to the results of Decheyne et al.³⁰ except that the magnitude of the ζ -potential versus pH data for the current study are uniformly greater. Decheyne et al. report electrophoretic measurements as positive, varying from 0 to 10mV³⁰. This variation is attributed to differences in particle size. The current study used crystalline, stoichiometric sieved powders having a mean diameter of $2.91\mu\text{m}$ while Decheyne et al.³⁰ used $<5\mu\text{m}$ crystalline, stoichiometric HA powders. Although these particle size differences may appear minor, as previously noted, the magnitude of the ζ -potential is indirectly proportional to the particle diameter through the inertial correction factor $G(\alpha)^{-1}$ as shown in Equation 3. The somewhat larger particle sizes used by Decheyne et al.³⁰ would yield ζ -potentials that are smaller in magnitude.

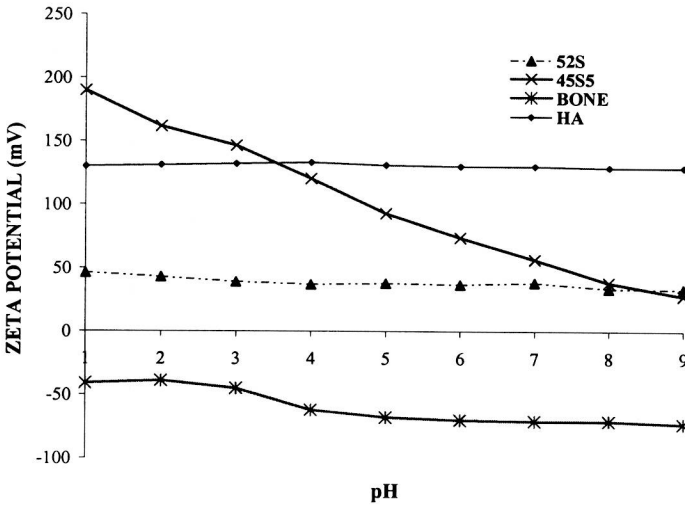


Figure 1: Zeta Potential versus pH for Bone, HA, 45S5 bioglass, and 52S Bioglass from electroacoustic measurements with an electrolyte concentration of 0.154M NaCl and solids content of 0.002%, respectively.

The ζ -potential of the bone varies from -40 to -48 mV throughout the pH range tested. Kowalchuk et al.²⁵ and Guzelsu et al.³¹ studied the ζ -potential of bovine bone using electrophoretic measurements and reported negative values with magnitudes ranging between 0 and 15mV. The lesser ζ -potential value is attributed to differences in particle size and size distribution, bone species, and measurement technique. Kowalchuk et al.²⁵ reported bone particle diameters as

<5 μ m, while Guzelsu et al.³¹ report particle diameters <10 μ m. The magnitude of the ζ -potential is indirectly proportional to the particle diameter as discussed earlier. Therefore the larger particle sizes of the powders used by Kowalchuk et al.²⁵ and Guzelsu et al.³¹ account for the lower ζ -potential measurements. Finally, differences in the ζ -potential values may be attributed to differences between bovine and the deer bone used in this study.

Stability Predictions

The stability factor, W, was next calculated for the composite systems (45S5/bone, 52S/bone, HA/bone) using ζ -potential data and plotted as log (W) verses pH in Figures 2-4, respectively. Using a potential barrier of >20 kT to indicate stability, a stability ratio of log (W)>~10 indicates a system which is stable with respect to agglomeration²⁴. The stability of the 45S5 Bioglass/bone system is shown in Figure 2 which illustrates that while the individual components (Bioglass and bone) are predicted to remain unagglomerated, the

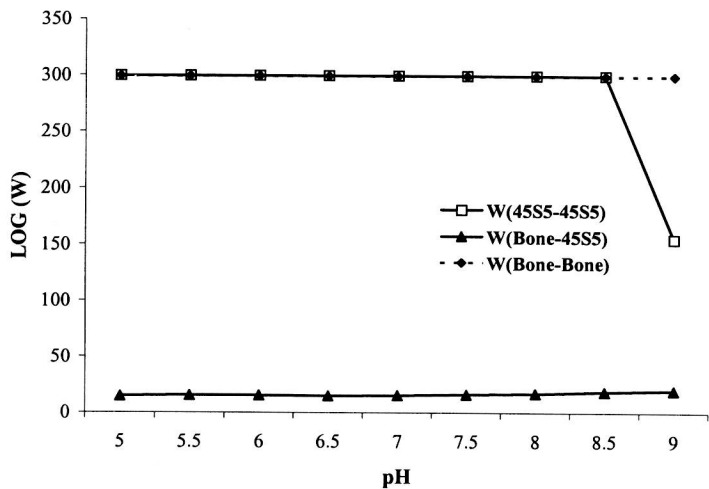


Figure 2: Stability ratio versus pH for bone/45S5 Bioglass using acoustophoretic ζ -potential data at T=30°C.

combination of bone and 45S5 Bioglass are predicted to agglomerate over the pH range tested. In contrast, the higher SiO₂ content 52S Bioglass/bone system shown in Figure 3 shows stability of the individual components and predicts no heteroagglomeration between the components. This agrees with clinical findings that link lower Ca to P molar ratios to a decrease in Bioglass/bone bonding³². The

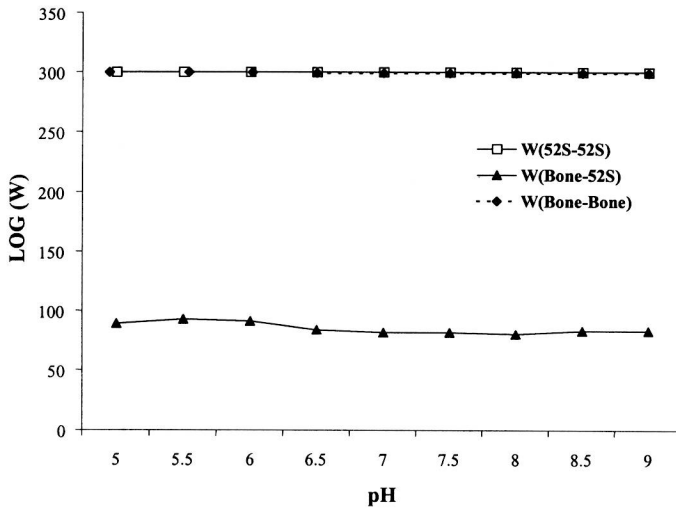


Figure 3: Stability ratio versus pH for bone/52S Bioglass using acoustophoretic ζ -potential data at $T=30^{\circ}\text{C}$.

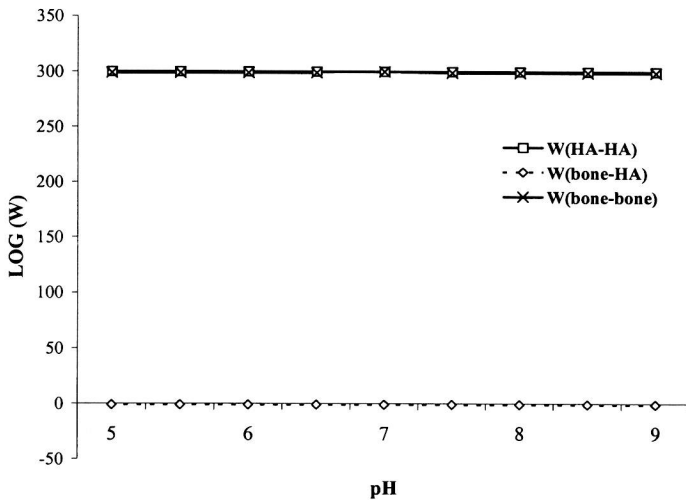


Figure 4: Stability ratio versus pH for bone/HA using acoustophoretic ζ -potential data at $T=30^{\circ}\text{C}$.

HA/bone system shown in Figure 4 illustrates that both the HA and the bone are stable/unagglomerated with respect to themselves throughout the pH range (5 to

10). However, the composite heterostability shows low, negative values over the pH range investigated. This negative log W value does not correspond to negative stability. Zero stability is the lowest possible stability state. Negative values are an artifact of taking the log of a small stability value. Therefore, from these results, it is expected that HA will agglomerate to bone from pH 5-10.

DISCUSSION

As discussed in an earlier paper³³, the instability of the HA/bone interaction coincides with the mechanisms for physicochemical HA/bone bonding, presented by Bagambisa et al.⁹. Here, the structure of both HA and canine bone are directed by the same calcium and phosphate ionic species present in the calcium phosphate rich layer at the implant surface. Thus, the HA/bone bond must involve strong ionic bonding between these two species. In TEM studies by Bagambisa et al.⁹, crystallites of bone were observed to directly bond to the HA surface. Direct HA to bone bonding agrees with the findings of this study which delineated the strong, unstable interaction between HA and bone, resulting in coagulation between these two materials. The heterocoagulation represents a stable interaction whereby the bone-HA interface lies at a thermodynamically lower energy state. The presence of such a stable bonding state predicts a strong mechanical bond since the inherent strength of any material is dependent upon the type and strength of its bonds.

This heterocoagulation behavior over the entire pH range is also significant when the *in vivo* behavior of this system is considered. Normal blood pH is approximately 7.4. In the immediate area around a wound, the pH may be significantly less, creating an acidic environment.

In comparing the ζ -potential versus pH measurements from Decheyne et al.³⁰ (HA), Kowalchuk et al.²⁵ (bone) and Guzelsu et al.³¹ (bone), the similar appearance of the curves is noted. While differences in the magnitude and sign of the ζ -potential of bone and HA are found to be a function of the particle size, stability calculations invariably indicate an unchanging, unstable interaction between bone and HA at all pHs. This differs from the experimental results of Bagambisa et al.⁹ that correlates the bonding zone thickness between bone and HA with changes in pH. For example, at pH 5.19, the HA-bone interaction layer increased but was subsequently resorbed as the pH returned to normal levels. This suggests that while ionic activity may dominate the HA-bone interaction, the cellular *in vivo* environment also plays a role in determining the extent of the initial HA-bone interaction layer.

CONCLUSIONS

Acoustophoretic particle potentials for bone and the synthetic implant materials 45S5 and 52S Bioglass, were measured as a function of pH and